

# Nanoscale

Accepted Manuscript



This is an *Accepted Manuscript*, which has been through the Royal Society of Chemistry peer review process and has been accepted for publication.

*Accepted Manuscripts* are published online shortly after acceptance, before technical editing, formatting and proof reading. Using this free service, authors can make their results available to the community, in citable form, before we publish the edited article. We will replace this *Accepted Manuscript* with the edited and formatted *Advance Article* as soon as it is available.

You can find more information about *Accepted Manuscripts* in the [Information for Authors](#).

Please note that technical editing may introduce minor changes to the text and/or graphics, which may alter content. The journal's standard [Terms & Conditions](#) and the [Ethical guidelines](#) still apply. In no event shall the Royal Society of Chemistry be held responsible for any errors or omissions in this *Accepted Manuscript* or any consequences arising from the use of any information it contains.

## COMMUNICATION

# Continuous fabrication of scalable 2-dimensional (2D) micro- and nanostructures by sequential 1D mechanical patterning processes

Cite this: DOI: 10.1039/x0xx00000x

Received 00th January 2014,  
Accepted 00th January 2014

DOI: 10.1039/x0xx00000x

[www.rsc.org/](http://www.rsc.org/)

Jong G. Ok,<sup>abc\*</sup> Ashwin Panday,<sup>d</sup> Taehwa Lee<sup>b</sup> and L. Jay Guo<sup>bcd\*</sup>

**We present a versatile and simple methodology for continuous and scalable 2D micro/nano-structure fabrication via sequential 1D patterning strokes enabled by Dynamic Nano-Inscribing (DNI) and Vibrational Indentation Patterning (VIP) as well as a ‘single-stroke’ 2D patterning by using a DNI tool in VIP.**

Beyond the uniaxial nanostructures such as nanogratings or one-dimensional (1D) nanomaterials (e.g., nanowires and nanotubes), multi-dimensional nanoarchitectures integrating micro/nano-scale features have become prevalent and their applications have permeated into many interdisciplinary fields.<sup>[1]</sup> For instance, the nanostructured three-dimensional (3D) scaffolds have been applied to tissue-engineering frameworks<sup>[2]</sup> and terahertz (THz) metamaterials.<sup>[3]</sup>

In particular, in-plane two-dimensional (2D) patterns are more favourable for integration into the thin-film structures and device fabrications, compared to vertically-grown 1D arrays or 3D complex structures. In the past decade, these planar 2D micro/nano-patterns have been utilized in a myriad of applications ranging from functional films (e.g., antireflection coatings,<sup>[4]</sup> plasmonic surfaces,<sup>[5]</sup> photonic color filters,<sup>[6, 7]</sup> and bioengineering templates<sup>[8]</sup>) to thin-film devices (e.g., lighting sources,<sup>[9, 10]</sup> organic optoelectronics,<sup>[11]</sup> and photovoltaics<sup>[12]</sup>). 2D micro/nano-patterns can be fabricated using techniques such as laser interference lithography (LIL)<sup>[5, 10, 13]</sup> or e-beam lithography (EBL)<sup>[4, 6, 14]</sup> typically accompanied by reactive ion etching. However, the process throughput and the scalability are limited, especially when the cost factor is taken into account. Alternative methods involving unconventional lithography have been investigated, for example, by adopting the self-assembled monolayers of block copolymers<sup>[15]</sup> and colloidal nanospheres<sup>[16]</sup> or porous anodized aluminium oxide slices<sup>[17]</sup> as 2D pattern masks. Further, more complex 2D patterning

techniques have also been developed by capitalizing specific optical patterns (e.g., Moiré pattern<sup>[18]</sup> and holographic pattern<sup>[19]</sup>) or modifying conventional lithography systems (e.g., phase-shift lithography,<sup>[20]</sup> 3-beam LIL,<sup>[21]</sup> evanescent wave-aided LIL<sup>[22]</sup>), or by delicate direct-write photolithography.<sup>[23]</sup> Nevertheless, various issues associated with pre- and post-treatment steps, tricky procedures, and/or lack of scalability impede more productive manufacturing and broader application of 2D micro/nano-patterns. Therefore, a simpler and more scalable 2D micro/nano-patterning process is highly desirable. Fabrication throughput as well as potential scalability will be significantly improved if such 2D patterns can be continuously and directly ‘written’ on substrates without resorting to mask preparation, complex lithography apparatus, and/or additional manipulation (e.g., annealing, etching, and mask stripping). Recently developed continuous mechanical nanopatterning methods,<sup>[24]</sup> such as dynamic nanoinscribing (DNI)<sup>[25]</sup> and vibrational indentation patterning (VIP),<sup>[26]</sup> enable the continuous and high-speed fabrication of micro/nano-grating patterns with simple setups and no needs of intricate masks; DNI inscribes and VIP indents 1D micro/nano-scale grating patterns very easily on flexible substrates. In this work, by a unique combination of these 1D patterning techniques we present a versatile but simple methodology for the continuous and scalable ‘direct-writing’ of 2D micro/nano-patterns. We also demonstrate a ‘single-stroke’ 2D patterning by adapting the grating-containing DNI tool as a vibrating edge in the VIP process. Since both DNI and VIP are fully capable of period control, a variety of large-area 2D patterns of desired dimensions can be continuously written on any substrates softer than the writing tool. Various applications requiring 2D micro/nano-patterns with good scalability and reproducibility can make use of this method. We demonstrate one specific use of the fabricated 2D nanopatterns: a size-selective capture and confinement of nanoparticles (NPs) in solution.

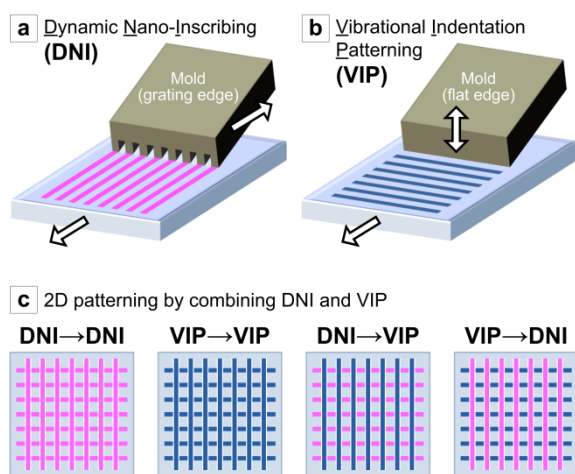


**Figure 1.** Schematics of scalable and high-throughput 2D patterning by combining continuous 1D nanograting fabrication techniques. Principles of (a) DNI and (b) VIP where the 1D nanogratings can be continuously fabricated over the large area by dynamic inscribing of a grating mould edge in DNI and periodic vibration of a flat tool edge in VIP. (c) Four combinations of DNI and VIP for 2D patterning: DNI+DNI (2D-DNI), VIP+VIP (2D-VIP), DNI then VIP, and VIP then DNI. The figures depict 90°-angled two sequential processes of DNI and VIP, but the 2D patterning can also be done in any arbitrary oblique angles.

**Figure 1a and 1b** depicts the typical 1D DNI and VIP processes, respectively. DNI uses the sharp edge of a hard grating mould to inscribe the pattern by plastically deform the polymer substrate. The mould edge can be locally heated to control the degree of plastic deformation of the substrate at contact, thereby tailoring the resulting pattern geometry.<sup>[25]</sup> VIP utilizes vertical vibration of a flat and sharp edge of a rigid tool, which makes periodic indentations into a moving substrate with a controlled gap from the tool. The period control in VIP is

possible simply by adjusting the vibration frequency and/or substrate moving speed.<sup>[26]</sup>

A variety of 2D patterns can be easily created by combining these two processes: DNI+DNI, VIP+VIP, DNI then VIP, and VIP then DNI, as schematically illustrated in **Figure 1c**. We are able to perform all the 2D patterning processes on as-received, commonly available flexible polymers such as polyethylene terephthalate (PET), polycarbonate (PC), and perfluoroalkoxy (PFA), illustrating the generality of the approach. For easier characterizations (e.g., cleaving to expose cross-sections for scanning electron microscopy (SEM) imaging), the fabricated polymer patterns are transferred onto Si wafers by using UV-curable epoxysilicone resin.<sup>[27]</sup> All pattern SEM images shown hereafter (unless otherwise specified) are taken from such transferred samples with inverted profiles.

The DNI process is straightforward (**Figure 1a**). We prepare the well-cleaved mould containing the desired pattern along the edge, bring the mould edge in contact with the substrate at a proper angle, apply a slight normal force and local heating to the mould if necessary, and then slide the mould edge over the substrate with the conformal contact maintained. As a result, the pattern is continuously inscribed on a substrate without seams until the process stops. Here the actual patterning occurs at the contacted “line”, thereby requiring very little force. A unique feature is that DNI enables indefinite large-area patterning irrespective of the original mould area.

2D patterning via DNI (denoted as 2D-DNI hereafter) is easily accomplished by performing two DNI processes in series along orthogonal directions or any oblique angles. **Figure 2** shows the SEM images of 2D nanopatterns fabricated by 2D-DNI. The first DNI-patterned grating can be slightly deformed by the second DNI patterning as DNI relies on the conformal contact throughout the inscribing stroke. However, since the mould openings do not touch the patterned surface during the second DNI, the overall 2D “waffle-like” patterns emerge.

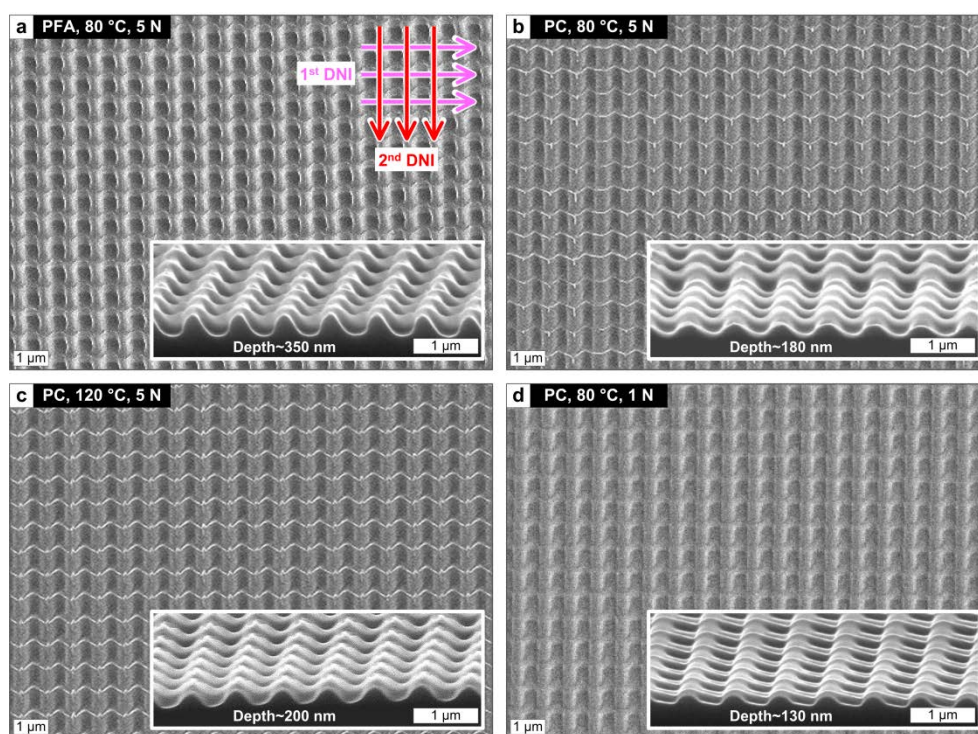


**Figure 2.** SEM images of 2D-DNI patterning results obtained in various process conditions and substrate materials. Substrate materials, DNI processing temperature, and mould loading forces are (a) PFA, 80 °C, 5 N, (b) PC, 80 °C, 5 N, (c) PC, 120 °C, 5 N, and (d) PC, 80 °C, 1 N, respectively (all top views). The inscribing directions for the 1<sup>st</sup> and 2<sup>nd</sup> DNI processes are marked in the upper right corner of (a), which apply to all the other three as well. Insets show the cross-sections with the measured pattern depths (all 45°-tilted views).

In DNI, the pattern period is dictated by that of the grating mould. For instance, we use a 700 nm period SiO<sub>2</sub> mould for the 700 nm-period patterning in this work (unless otherwise noted). Furthermore, the morphologies of the 2D nanopatterns created by 2D-DNI can be specifically tailored by changing the substrate material, applied force, and processing temperature. For example, a 350 nm-deep pattern (**Figure 2a**) can be formed at 80 °C under 5 N load for soft PFA (Young's modulus  $E \approx 0.5$  GPa), compared to one with the 180 nm depth (**Figure 2b**) using a relatively hard PC ( $E \approx 2.3$  GPa) under identical force and temperature. For the same PC substrate material, increasing the processing force and temperature deepens the pattern profiles (**Figure 2b-d**). The DNI pattern profile largely depends on the plastic deformation of a substrate induced by the mechanical stress from the edge of the mould under conformal contact. Hence, polymers that have a certain level of compliance, relatively low modulus, and a reasonable glass transition temperature ( $T_g$ ; PFA~90°C, PC~140°C), are best suited for DNI substrates. In this way, the modulation of mechanical force and processing temperature at the mould-substrate contact zone allows us to control the degree of substrate deformation, namely, the final 2D pattern topology.

Next, we consider the VIP process (**Figure 1b**) and its utilization in 2D patterning. VIP is even more economical than DNI as it does not require any pre-fabricated moulds. By vertically vibrating a flat, sharply-cleaved tool edge (e.g. Si<sub>3</sub>N<sub>4</sub>) tilted at the desired angle (e.g. 45°) over a horizontally-moving substrate with lesser hardness, periodic gratings or lines with arbitrary spacings can be 'indented' in a continuous manner. Following this, we can produce 2D patterns via two sequential VIP processes (2D-VIP), for example, along the perpendicular directions at identical frequency and force to make uniform square mesh patterns as reported in our previous work.<sup>[26]</sup> **Figure 3a** shows more unique 2D-VIP patterns on PET, comprising the different pattern depths along each direction but with the same period of ~5 μm; further examples of different

depths and periods are demonstrated in **Figure 3b-d** below. The VIP pattern period and depth can be controlled by regulating the vibration frequency ( $f$ ), substrate feeding speed ( $V$ ), vibration amplitude ( $z$ ), and mould-substrate gap ( $g$ ); for the 45°-tilted tool vibration, the pattern period  $\lambda$  and depth  $d$  are given as  $\lambda = V/f$  and  $d = z - g$ , respectively. For instance, the 5 μm-period 2D-VIP pattern shown in **Figure 3a** results from  $f = 50$  Hz (3000 rpm) and  $V = 250 \mu\text{m s}^{-1}$ . Similar to DNI, compliant polymers are useful as the substrate materials because the conformal line contact between the vibrating mold edge and underlying substrate surface is preferred for uniform line indentations. The patterning principle and resulting profile of this 2D-VIP are similar to the previously demonstrated 2D micropatterns made by repeated indentations of a sharp blade driven by XYZ stage,<sup>[28]</sup> but 2D-VIP is much faster and easier because it uses high-frequency vibration instead of slow precision stage control.

DNI and VIP can also be 'mixed' for 2D patterning. **Figure 3b-d** exemplifies the 2D patterns made by DNI/VIP combination. Here the processing conditions of DNI and VIP can be independently controlled to determine the final 2D pattern topology. For example, the DNI grating can turn into the 2D pattern by bearing VIP grooves across the grating direction (**Figure 3b**). Also, a shallow DNI (1 N force) can be done over the 3 μm-period VIP patterns of various depths (**Figure 3c**), or a deep DNI process (5 N force) can be coupled with a shallow, 7 μm-period VIP pattern DNI process (**Figure 3d**), and so on.

Continuously creating the 2D patterns with a 'single' stroke is further beneficial for improving fabrication throughput. This can be done in VIP by adopting the cleaved nanograting edge as a vibrating tool. This grating-vibrational indentation patterning process (G-VIP) naturally indents 2D patterns (**Figure 4a**). The resulting pattern morphology can be realized in various shapes by controlling the G-VIP process parameters and substrate materials as demonstrated in **Figure 4b-c**; here we regulate substrate velocity  $V$  under the same vibration

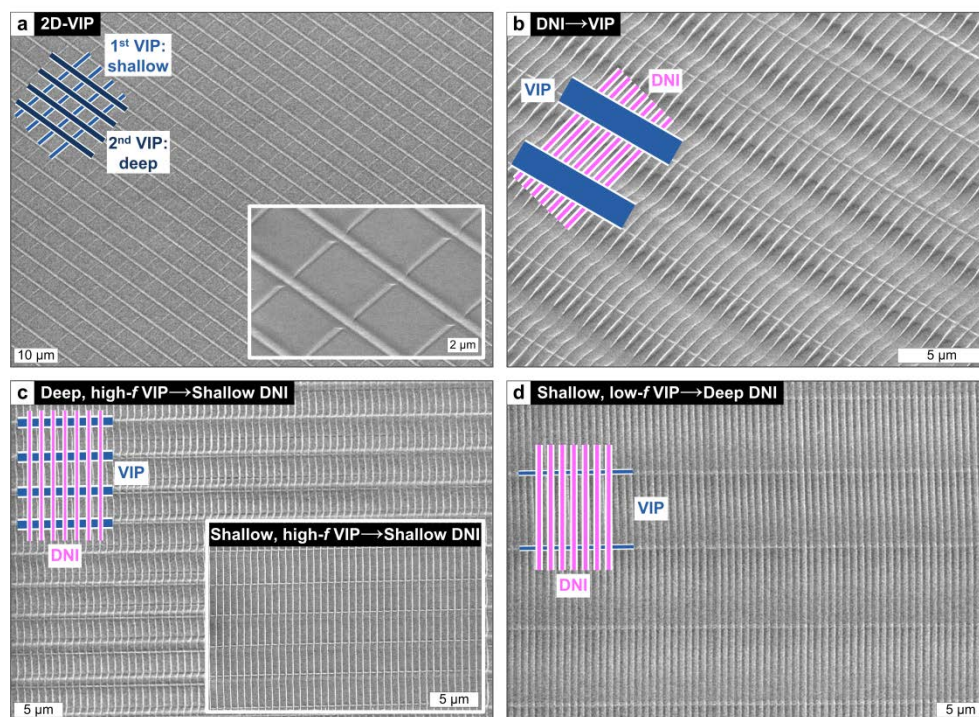


**Figure 3.** SEM images of various 2D patterns fabricated by (a) 2D-VIP (45°-tilted view) on PET, (b) DNI then VIP (45°-tilted view) on PC, and (c-d) VIP then DNI under different conditions on PC (top views). The processing temperatures of VIP and DNI were room temperature and 120 °C, respectively. Schematic drawings of patterning sequences are illustrated in the upper left corners of each figure. Inset to Figure (a) (45°-tilted view) shows an enlarged view of the 2D-VIP pattern, where two dented gratings with different depths can be clearly seen.

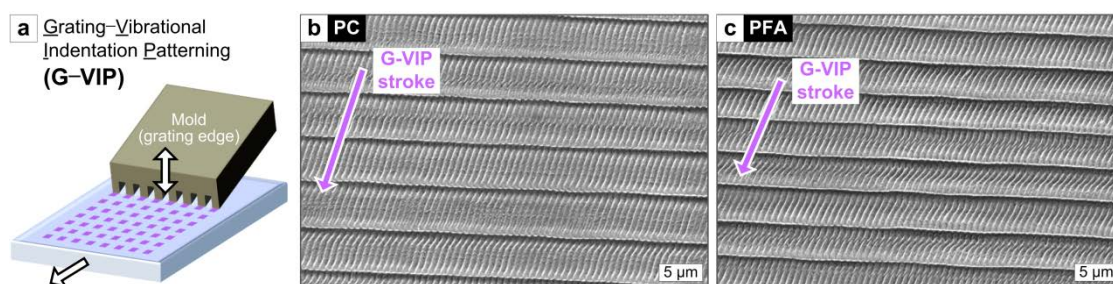


**Figure 4.** One-step fabrication of 2D patterns by G-VIP. (a) Schematics of G-VIP where a grating mould edge makes periodical indentations over the moving substrates to realize 2D patterns in one stroke. SEM images of G-VIP patterns fabricated on (b) PC and (c) PFA substrates with G-VIP stroke direction mark-ups.

frequency  $f$  for period control: 5  $\mu\text{m}$  for PC (**Figure 4b**) and 3.5  $\mu\text{m}$  for PFA (**Figure 4c**). It can be seen that PFA having lower  $E$  than PC yields deeper pattern profile for both DNI-driven grooves and VIP-driven indentations at the identical vibration condition, which is consistent with the mechanisms of DNI and VIP discussed above.

From a manufacturing standpoint, it is always desirable to have targeted multi-dimensional micro/nano-scale features that can be scaled up to large areas at low cost and high throughput. All 2D patterning methodologies presented in this work can be potentially beneficial in this regard. For instance, all that is required in VIP is a flat sharp edge. The DNI grating mould preparation itself requires typical patterning such as nanoimprinting,<sup>[29]</sup> but once a mould is prepared on a cleavable substrate such as a Si wafer, numerous pieces of DNI tools can be obtained from a single wafer. Once the edge becomes dull due to repeated use, one can re-cleave it to expose a fresh grating edge. In our DNI condition, the mould re-cleaving can be done in about every 5 m patterning stroke. A potential use of the 2D patterns generated by the combinations of DNI and VIP is that they can be used as large area mould in the roll-to-roll nanoimprint patterning process.<sup>[30]</sup> The underlying nature of plastic deformation in DNI and VIP recommends the use of compliant polymers as the target substrate materials, yet the as-fabricated pattern can be easily metallized or transferred to desired substrates for subsequent uses.

The 2D DNI/VIP combination triggers facile and high-throughput manufacturing of templates and components that can be used for a multitude of applications ranging from electronics and photonics to energy conversion and bioengineering. Large-area patterns are a primary requirement for high throughput biological applications like filtration or particle manipulation systems.<sup>[31]</sup> In particular, the 2D-DNI process enables the large-area fabrication of complex planar nanostructures such as a 2D sinusoidal ‘void’ pattern (**Figure 5a**) that is capable of confining and manipulating charged micro/nano-scale entities including NPs, lipid vesicles, cancer cells, and bacteria. We experimentally demonstrate this application by using colloidal polystyrene NPs. Advancements in the field of colloidal synthesis have spurred the usage of NPs in drug delivery systems, optoelectronic devices, photovoltaics, and filtration.<sup>[32]</sup> Many of these technologies would greatly benefit from a selective 2D spatial confinement of NPs into organized structures. Although strategies involving directed self-assembly have been studied extensively in the past,<sup>[33]</sup> selective placement and organization of NPs on the various types of substrates and over large areas remains a challenge. Using a combination of electrostatic interactions and our 2D patterning technique, we have created a single-step methodology to selectively confine and pattern NPs on flexible substrates.

Colloidal particles assemble into arrays whose order depends closely on the relative dimensions of the spheres and the pattern as well as the pattern geometry. Our process is based on generating a sinusoidal electrostatic potential on the 2D-DNI-patterned substrate that has the ability to couple with oppositely charged colloidal NPs in ionic solution. Most macromolecules as well as many oxide surfaces develop a net electric charge (by either the dissociation of chemical groups or the adsorption of ions from solution) when suspended in an ionic solution.<sup>[34]</sup> The charged NPs undergoing Brownian motion in solution experiences an electrostatic attraction in the vicinity of the oppositely charged surface.<sup>[35]</sup> When the surface is patterned into voids of the specific size, the size-dependent confinement of NPs is induced inside the nanoscale voids.

Our experimental device consists of a microfluidic cell chamber consisting of two transparent cover slips held at a separation of 1 mm by polydimethylsiloxane (PDMS) spacers (**Figure 5b**). One of these cover slips contains the 2D array of 2D-DNI-patterned 700 nm-pitched voids coated with 10 nm-thick  $\text{Al}_2\text{O}_3$  which is positively charged when immersed in aqueous NaCl solution (osmotic zeta potential<sup>[36]</sup> of  $+2.1 \text{ e nm}^{-2} \sim$  surface charge density of  $+23 \text{ mV}$ ). The other acts as a transparent medium for microscopic characterization. As the suspension of negatively charged polystyrene NPs ( $-1.8 \text{ e nm}^{-2} \sim -56 \pm 13 \text{ mV}$ ) is flown into the fluidic cell, their size and surface charge density dictate the trapping behaviour.

We directly visualize the instantaneous confinement and assembly of fluorescently labelled 500 nm-diameter polystyrene particles in the patterned voids (**Figure 5c**). The 2D sinusoidal potential profile accentuates the trapping process, enabling the size specificity of this confinement methodology. Densification can be increased by further optimization which is underway. The methodology described here is substrate-independent and contains a greater number of voids/unit area compared to conventional methods. By controlling the pitch and depth of the 2D void pattern, its electrostatic potential profile can be tuned to accommodate specificity, trapping, and organization of various-sized micro/nano-scale entities, which broadens its applications in high-throughput filtration and separation systems. Detailed investigation supported by analytic modelling is needed and is in progress.

In summary, we have presented the facile, cost-effective, and easily scalable manufacturing of 2D micro/nano-patterns by creatively applying the continuous 1D grating fabrication techniques such as DNI and VIP in multiple directions. Since both DNI and VIP are based on mechanical deformation and fully capable of period control, the 2D patterns of various morphologies can be readily obtained through the combination of DNI and VIP as well as G-VIP on any substrate that is softer than the tool. Among many potential applications, we demonstrate the use of such fabricated 2D patterns for the

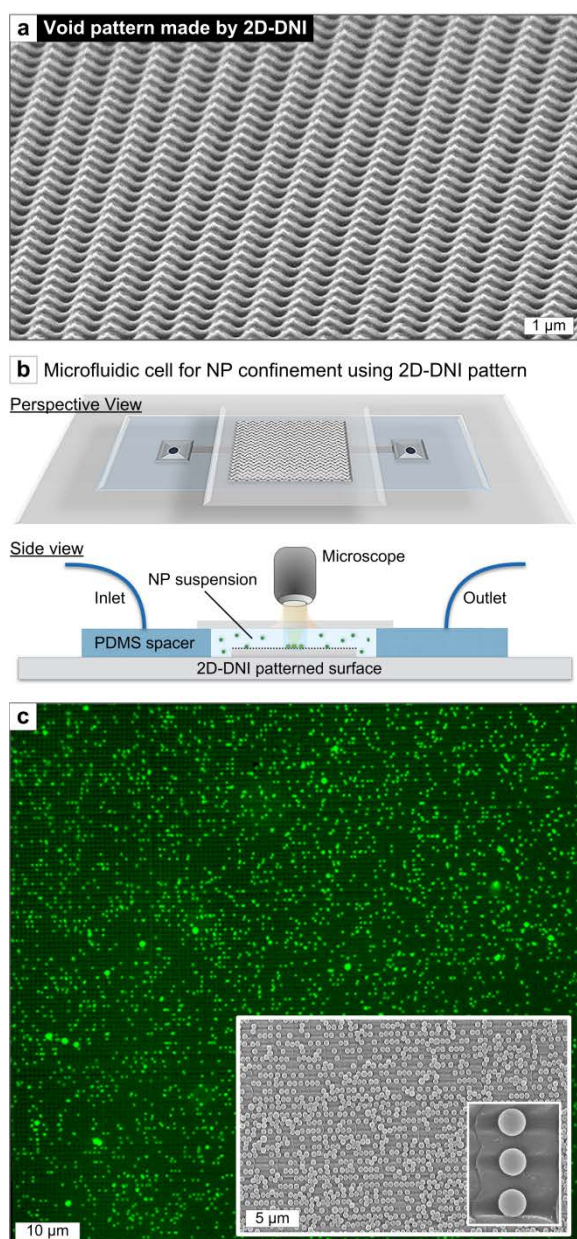


**Figure 5.** Application of the 2D-DNI pattern in NP trapping and confinement. (a) SEM image of 700 nm-period 2D 'void' pattern formed on a PC substrate by 2D-DNI. (b) Schematics of a microfluidic cell containing the 2D-DNI pattern coated with 10 nm-thick  $\text{Al}_2\text{O}_3$ . A suspension of 500 nm-diameter polystyrene NPs is injected into the cell immersed in NaCl solution, while a microscope monitors and records the motion of NPs. (c) Epifluorescent microscope image of polystyrene NPs docked in the  $\text{Al}_2\text{O}_3$ -coated 2D-DNI pattern framework. Inset to (c) shows SEM images taken after the sample is dried, where the enlarged view in lower-right corner discloses three NPs confined in three grooves in series.

colloidal nanoparticle confinement, which could potentially lead to the sorting and trapping of various biological species including bacteria and circulating tumour cells. The excellent fabrication throughput of our method will facilitate the use of multi-dimensional micro/nano-patterns in many applications that require large areas.

### Experimental Section

**Processing:** Details of DNI<sup>[25]</sup> and VIP<sup>[26]</sup> processes along with mould preparation<sup>[37]</sup> and cleaving<sup>[38]</sup> procedure can be found

elsewhere. All polymer substrates (PET and PC from Tekra Corp., PFA from Saint-Gobain) were used as purchased or after IPA cleaning followed by nitrogen drying. For the NP confinement cell fabrication, a 2D-DNI-patterned PC substrate was coated with a 10 nm-thick  $\text{Al}_2\text{O}_3$  layer by RF sputtering (Lab 18-2, Kurt J. Lesker) and was put in the microfluidic cell chamber held at a separation of 1 mm by PDMS spacers between two transparent cover slips. This assembled cell was immersed in an ionic solution (0.1 mM [NaCl]), and then a small volume (~50  $\mu\text{L}$ ) of the polystyrene NP suspension at an initial volume fraction of 0.5 % wt was injected into the chamber. The ionic solution containing NPs was allowed to equilibrate inside the chamber for 5 minutes and then deionized water rinsing was applied to remove excess NPs.

**Characterization:** SEM imaging was performed using a Philips XL30-FEG at the typical operating voltage of 10–25 kV, after sputtering a thin Au film ( $\approx 3$ –5 nm) to avoid electron charging. For NP confinement visualization, fluorescently labelled (FITC 505/515nm) NPs were used and the device was examined on an epifluorescent microscope (Nikon TE-2000, NA=1.4). A Zetasizer Nano (Malvern Instruments) was used to measure zeta potentials.<sup>[34]</sup>

### Acknowledgements

This study was supported by the National Science Foundation (DMR-1120187) and Seoul National University of Science and Technology. Electron microscopy was performed at the University of Michigan Electron Microbeam Analysis Laboratory (EMAL). Microfabrication was performed at the University of Michigan Lurie Nanofabrication Facility (LNF).

### Notes and references

- <sup>a</sup> Department of Mechanical and Automotive Engineering, Seoul National University of Science and Technology, Seoul, 139-743, Korea.  
<sup>b</sup> Department of Mechanical Engineering, University of Michigan, Ann Arbor, MI 48109, USA.  
<sup>c</sup> Department of Electrical Engineering and Computer Science, University of Michigan, Ann Arbor, MI 48109, USA.  
<sup>d</sup> Macromolecular Science and Engineering, University of Michigan, Ann Arbor, MI 48109, USA.  
 \* Corresponding Authors: jgok@seoultech.ac.kr, guo@umich.edu.

- 1 T. G. Leong, A. M. Zarafshar, D. H. Gracias, *Small*, 2010, **6**, 792; L. Jiang, X. Wang, L. F. Chi, *Small*, 2011, **7**, 1309; X. Z. Ye, L. M. Qi, *Nano Today*, 2011, **6**, 608; S. Tawfick, M. De Volder, D. Copic, S. J. Park, C. R. Oliver, E. S. Polsen, M. J. Roberts, A. J. Hart, *Adv. Mater.*, 2012, **24**, 1628.
- 2 H. D. Cha, J. M. Hong, T. Y. Kang, J. W. Jung, D. H. Ha, D. W. Cho, *J. Micromech. Microeng.*, 2012, **22**, 9.
- 3 H. O. Moser, C. Rockstuhl, *Laser Photonics Rev.*, 2012, **6**, 219.
- 4 Y. Kanamori, H. Kikuta, K. Hane, *Jpn. J. Appl. Phys.*, 2000, **39**, L735; Y. Kanamori, M. Ishimori, K. Hane, *IEEE Photonics Tech. Lett.*, 2002, **14**, 1064.
- 5 J. Li, H. Iu, W. C. Luk, J. T. K. Wan, H. C. Ong, *Appl. Phys. Lett.*, 2008, **92**, 213106; H. Iu, J. Li, H. C. Ong, J. T. K. Wan, *Opt. Express*, 2008, **16**, 10294.
- 6 E. H. Cho, H. S. Kim, B. H. Cheong, P. Oleg, W. Xianyua, J. S. Sohn, D. J. Ma, H. Y. Choi, N. C. Park, Y. P. Park, *Opt. Express*, 2009, **17**, 8621; E. H. Cho, H. S. Kim, J. S. Sohn, C. Y. Moon, N. C. Park, Y. P. Park, *Opt. Express*, 2010, **18**, 27712.

- 7 S. Landis, P. Brianceau, V. Reboud, N. Chaix, Y. Desieres, M. Argoud, *Microelectron. Eng.*, 2013, **111**, 193.
- 8 V. N. Truskett, M. P. C. Watts, *Trends Biotechnol.*, 2006, **24**, 312; J. J. Amsden, P. Domachuk, A. Gopinath, R. D. White, L. Dal Negro, D. L. Kaplan, F. G. Omenetto, *Adv. Mater.*, 2010, **22**, 1746; M. Tanaka, *Biochim. Biophys. Acta-Gen. Subjects*, 2011, **1810**, 251.
- 9 S. Moller, S. R. Forrest, *J. Appl. Phys.*, 2002, **91**, 3324; Y. Sun, S. R. Forrest, *Nature Photon.*, 2008, **2**, 483; T. W. Koh, J. M. Choi, S. Lee, S. Yoo, *Adv. Mater.*, 2010, **22**, 1849.
- 10 Y. C. Kim, Y. R. Do, *Opt. Express*, 2005, **13**, 1598.
- 11 L. Petti, M. Ripa, R. Capasso, G. Nenna, A. D. Del Mauro, G. Pandolfi, M. G. Maglione, C. Minarini, *ACS Appl. Mater. Interfaces*, 2013, **5**, 4777.
- 12 M. M. Hilali, S. Q. Yang, M. Miller, F. Xu, S. Banerjee, S. V. Sreenivasan, *Nanotechnology*, 2012, **23**, 405203.
- 13 X. L. Chen, S. H. Zaidi, S. R. J. Brueck, D. J. Devine, *J. Vac. Sci. Tech. B*, 1996, **14**, 3339.
- 14 J. Nishii, K. Kintaka, Y. Kawamoto, A. Mizutani, H. Kikuta, *J. Ceram. Soc. Jpn.*, 2003, **111**, 24.
- 15 D. G. Choi, H. K. Yu, S. M. Yang, *Mat. Sci. Eng. C-Bio. S.*, 2004, **24**, 213.
- 16 W. Wu, A. Katsnelson, O. G. Memis, H. Mohseni, *Nanotechnology*, 2007, **18**, 485302; H. K. Park, J. H. Moon, S. Yoon, Y. R. Do, *J. Electrochem. Soc.*, 2011, **158**, J143; G. Perotto, A. Antonello, D. Ferraro, G. Mattei, A. Martucci, *Mater. Chem. Phys.*, 2013, **142**, 712; Z. Zhao, Y. J. Cai, W. S. Liao, P. S. Cremer, *Langmuir*, 2013, **29**, 6737; Y. Li, G. Duan, G. Liu, W. Cai, *Chem. Soc. Rev.*, 2013, **42**, 3614; Z. Dai, L. Jia, G. Duan, Y. Li, H. Zhang, J. Wang, J. Hu, W. Cai, *Chem. Eur. J.*, 2013, **19**, 13387.
- 17 K. Kim, J. Choi, M. Jung, D. H. Woo, *Jpn. J. Appl. Phys.*, 2008, **47**, 6354.
- 18 S. M. Lubin, W. Zhou, A. J. Hryn, M. D. Huntington, T. W. Odom, *Nano Lett.*, 2012, **12**, 4948.
- 19 M. Q. Lu, B. K. Juluri, Y. H. Zhao, Y. J. Liu, T. J. Bunning, T. J. Huang, *J. Appl. Phys.*, 2012, **112**, 113101; H. C. Jeon, C. J. Heo, S. Y. Lee, S. M. Yang, *Adv. Funct. Mater.*, 2012, **22**, 4268; I. Wathuthanthri, Y. Y. Liu, K. Du, W. Xu, C. H. Choi, *Adv. Funct. Mater.*, 2013, **23**, 608.
- 20 S. Jeon, V. Malyarchuk, J. A. Rogers, G. P. Wiederrecht, *Opt. Express*, 2006, **14**, 2300.
- 21 J. L. Stay, G. M. Burrow, T. K. Gaylord, *Rev. Sci. Instrum.*, 2011, **82**, 023115.
- 22 E. A. Bezus, L. L. Doskolovich, N. L. Kazanskiy, *Microelectron. Eng.*, 2011, **88**, 170.
- 23 H. L. Chen, K. T. Huang, C. H. Lin, W. Y. Wang, W. Fan, *Microelectron. Eng.*, 2007, **84**, 750.
- 24 J. G. Ok, S. H. Ahn, M. K. Kwak, L. J. Guo, *J. Mater. Chem. C*, 2013, **1**, 7681.
- 25 S. H. Ahn, L. J. Guo, *Nano Lett.*, 2009, **9**, 4392.
- 26 S. H. Ahn, J. G. Ok, M. K. Kwak, K. T. Lee, J. Y. Lee, L. J. Guo, *Adv. Funct. Mater.*, 2013, **23**, 4739.
- 27 X. Cheng, L. J. Guo, P. F. Fu, *Adv. Mater.*, 2005, **17**, 1419.
- 28 M. Yoshino, H. Ohsawa, A. Yamanaka, *J. Micromech. Microeng.*, 2011, **21**, 125017.
- 29 L. J. Guo, *Adv. Mater.*, 2007, **19**, 495.
- 30 S. H. Ahn, L. J. Guo, *Adv. Mater.*, 2008, **20**, 2044; S. H. Ahn, L. J. Guo, *ACS Nano*, 2009, **3**, 2304.
- 31 M. Václavíková, K. Vitale, G. P. Gallios, L. Ivanicová, *Water Treatment Technologies for the Removal of High-Toxicity Pollutants*, Springer, 2009.
- 32 M. A. S. Vigeant, R. M. Ford, M. Wagner, L. K. Tamm, *Appl. Environ. Microb.*, 2002, **68**, 2794; W. H. De Jong, P. J. A. Borm, *Int. J. Nanomed.*, 2008, **3**, 133; E. Stratakis, E. Kymakis, *Mater. Today*, 2013, **16**, 133.
- 33 F. Li, D. P. Josephson, A. Stein, *Angew. Chem. Int. Ed.*, 2011, **50**, 360.
- 34 A. L. Loeb, J. T. G. Overbeek, P. H. Wiersema, *The electrical double layer around a spherical colloid particle*, MIT Press, Cambridge, MA, USA, 1961.
- 35 M. Polin, D. G. Grier, Y. Han, *Phys. Rev. E*, 2007, **76**, 041406.
- 36 H. M. Park, S. M. Hong, J. S. Lee, *Biomed. Microdevices*, 2007, **9**, 751.
- 37 M. G. Kang, M. S. Kim, J. S. Kim, L. J. Guo, *Adv. Mater.*, 2008, **20**, 4408.
- 38 J. G. Ok, H. J. Park, M. K. Kwak, C. A. Pina-Hernandez, S. H. Ahn, L. J. Guo, *Adv. Mater.*, 2011, **23**, 4444.